Feature-Fusion-Based Haze Recognition in Endoscopic Images

Zhe Yu[1,2], Xiao-Hu Zhou[1,2(✉)], Xiao-Liang Xie[1,2], Shi-Qi Liu[1,2], Zhen-Qiu Feng[1,2], and Zeng-Guang Hou[1,2,3,4(✉)]

[1] The State Key Laboratory of Multimodal Artificial Intelligence Systems, Institute of Automation, Chinese Academy of Sciences, Beijing 100190, China
{yuzhe2021,xiaohu.zhou,zengguang.hou}@ia.ac.cn
[2] The School of Artificial Intelligence, University of Chinese Academy of Sciences, Beijing 100049, China
[3] The CAS Center for Excellence in Brain Science and Intelligence Technology, Beijing 100190, China
[4] The Joint Laboratory of Intelligence Science and Technology, Institute of Systems Engineering, Macau University of Science and Technology, Taipa, Macau

Abstract. Haze generated during endoscopic surgeries significantly obstructs the surgeon's field of view, leading to inaccurate clinical judgments and elevated surgical risks. Identifying whether endoscopic images contain haze is essential for dehazing. However, existing haze image classification approaches usually concentrate on natural images, showing inferior performance when applied to endoscopic images. To address this issue, an effective haze recognition method specifically designed for endoscopic images is proposed. This paper innovatively employs three kinds of features (i.e., color, edge, and dark channel), which are selected based on the unique characteristics of endoscopic haze images. These features are then fused and inputted into a Support Vector Machine (SVM) classifier. Evaluated on clinical endoscopic images, our method demonstrates superior performance: (Accuracy: 98.67%, Precision: 98.03%, and Recall: 99.33%), outperforming existing methods. The proposed method is expected to enhance the performance of future dehazing algorithms in endoscopic images, potentially improving surgical accuracy and reducing surgical risks.

Keywords: Endoscopic image · Haze recognition · Feature fusion

1 Introduction

Recent technological advancements in endoscopy have enabled surgeons to visualize surgical fields clearly during surgeries. Endoscopic images provide a view that is nearly equivalent to the surgeon's own eyes. However, some haze may be generated during surgical operations, which can obscure visibility and significantly affect a surgeon's ability to operate. Therefore, dehazing task for endoscopic images is necessary.

B. Luo et al. (Eds.): ICONIP 2023, CCIS 1966, pp. 375–387, 2024.
https://doi.org/10.1007/978-981-99-8148-9_30

Although many studies have focused on the dehazing task, existing image dehazing methods often ignore whether an image contains haze and are applied to the image directly. However, for endoscopic images, it is necessary to distinguish whether an image needs dehazing. This is important for two reasons: first, if the dehazing algorithm is used directly without judging whether the image contains haze, the resulting image may have lower visibility than the original image. Second, using the dehazing algorithm is time-consuming and can affect the real-time performance of endoscopic surgery images. Selectively using the dehazing algorithm can reduce the time required. Therefore, a haze image classification model is needed to improve the performance of dehazing algorithms.

Many studies have used traditional Machine Learning (ML)-based approaches to classify haze images. Yu *et al.* [16] extracted three features(image visibility, intensity of dark channel, and image contrast) and combined them with Support Vector Machine (SVM) to distinguish between haze and non-haze images. Zhang *et al.* [17] used the variance of HSI images as a feather and computed the angular deviation of different haze images compared to clear day images as another feature, they also used SVM for classification. Pal *et al.* [10] proposed a framework for image classification based on nine features and K-Nearest Neighbor (KNN) method. In [13], nineteen classification techniques were applied using five training parameters: area, mean, minimum intensity, maximum intensity, and standard deviation. Additionally, Wan *et al.* [15] used Gaussian Mixture Model to learn the probability density of three situations: non-haze, haze, and dense haze. The model's parameters were learned using the expectation-maximization algorithm.

Apart from traditional ML-based approaches, some methods are proposed based on Convolutional Neural Networks (CNN). Guo *et al.* [7] combined transfer learning and proposed a haze image classification method based on the Alexnet network transfer model. Pei *et al.* [11] proposed an end-to-end Consistency Guided Network, for classifying haze images. In [12], the authors proposed a deep neural network to identify haze images. Chincholkar *et al.* [5] presented the implementation of CNN to detect and classify the images into haze and non-haze based on the factors such as image brightness, luminance, intensity, and variance.

Existing methods usually focus on natural images, showing inferior performance when applied to endoscopic images. Therefore, this paper proposes a method to judge whether endoscopic images are haze or non-haze. The method implementation process is as follows: first, images are captured from different endoscopic surgery videos to form the training and test set. After extensive experimental analyses, three kinds of features including the color feature, the edge feature, and the dark channel feature are extracted from images in the training set and then fused together. An SVM model is trained to identify whether an image is haze or non-haze. The trained model is tested using features extracted from the test set and demonstrates high classification results.

The main contributions of this paper can be summarised as follows:

- Based on the unique characteristics of endoscopic haze images, three kinds of features (i.e., color, edge, and dark channel) are extracted from images and fused to distinguish between haze and non-haze endoscopic images.
- Various machine learning algorithms and fusion strategies based on the three kinds of features are experimented with the goal of optimizing the classification results.
- Extensive experiments demonstrate that our method can achieve a classification accuracy of 98.67% on endoscopic images, surpassing existing approaches.

The remainder of this paper is structured as follows: Sect. 2 depicts the proposed method. The experimental results are presented in Sect. 3. Section 4 discusses the advantages of our method. Finally, the conclusion of this paper is provided in Sect. 5.

2 Method

2.1 Features Extraction

In order to accurately distinguish between haze images and non-haze images, extracting appropriate features is the key point. This section introduces the three kinds of features extracted from images, which are the color feature, the edge feature, and the dark channel feature. All the features are fused to form the final feature.

Color Feature. Generally, haze can cause color changes in images, so the first kind of feature chosen is the color feature. There are two commonly used categories of color models: the hardware oriented and the color processing application oriented color model. The RGB color model is the most widely used hardware oriented color model owing to easily storing and displaying images on computers. However, the non-linearity with visual perception makes it unsuitable for this task. Therefore, the HSI color model, which is widely used in image processing applications, is chosen instead.

The HSI color model is based on hue, saturation, and intensity, which conforms to how people describe and interpret colors. Hue (H) represents the main pure color perceived by an observer with a range of angles between 0 and 2π. Red is represented by both 0 and 2π, green is represented by $2/3\pi$, and blue is represented by $4/3\pi$. Saturation (S), ranging from 0 to 1, refers to the relative purity of a color, or the amount of white light mixed with a color. Intensity (I) refers to the brightness of light, also ranging from 0 to 1, where black is represented by 0, and white is represented by 1. In contrast to the RGB color model, the HSI color model separates brightness and color information, making it more advantageous for endoscopic haze classification tasks. HSI values can be computed from RGB values as follows, where R, G, and B represent values of the three color channels in the image:

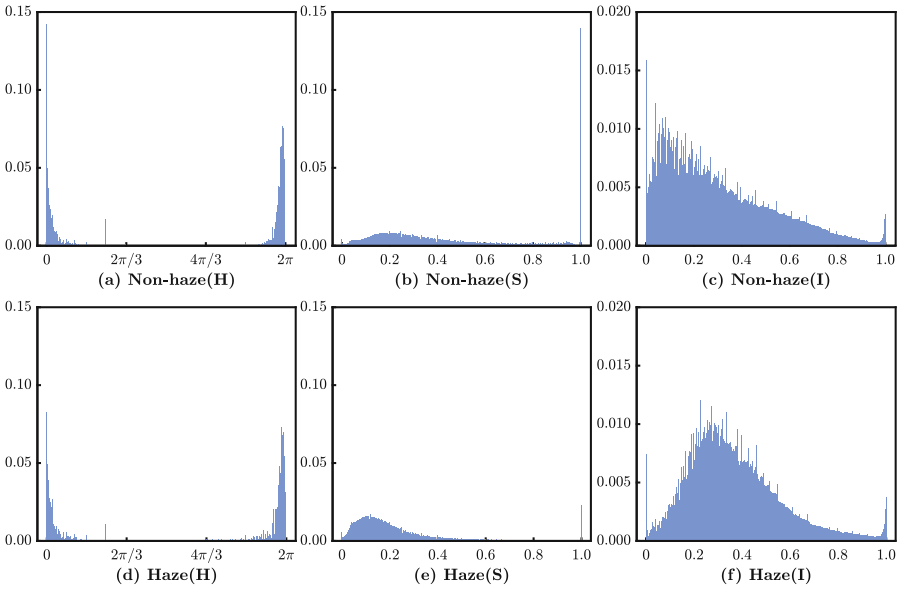

Fig. 1. The average HSI histograms of haze images and non-haze images.

$$\begin{cases} H = \begin{cases} \theta, & B \leq G \\ 2\pi - \theta, & B > G \end{cases} \\ S = 1 - \frac{3}{(R+G+B)} \left[\min\left(R, G, B\right)\right] \\ I = \frac{1}{3}\left(R + G + B\right) \end{cases} \tag{1}$$

$$\theta = \arccos\left\{ \frac{\frac{1}{2}\left[(R-G) + (R-B)\right]}{\left[(R-G)^2 + (R-B)(G-B)\right]^{\frac{1}{2}}} \right\} \tag{2}$$

Once the HSI color model is obtained, separate histograms are drawn for H, S, and I. Histograms can directly reflect the distribution of variables. Figure 1 shows the average H, S, and I histograms of 230 haze images and 270 non-haze images. Figure 1(a) and (b) show that haze changes the hue distribution. Non-haze images mainly contain a red hue owing to their origin in endoscopic surgery videos. In contrast, haze images exhibit a decreased ratio of pure red and a more dispersed hue distribution. Additionally, comparing Fig. 1(b) and (e), Fig. 1(c) and (f), it is evident that the haze also reduces saturation and increases intensity by adding more white light to images.

Edge Feature. One distinct feature for effectively distinguishing between haze and non-haze images is the image edge feature. Image edges contain rich information, the more details the edges of the image contain, the higher sharpness the image has. Moreover, haze reduces image sharpness and blurs image edges.

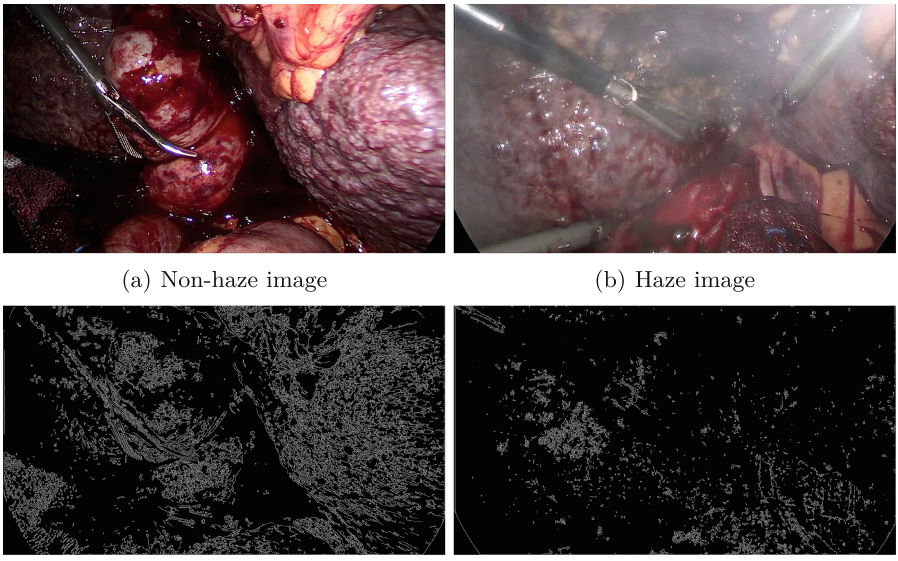

(a) Non-haze image (b) Haze image

(c) Edges of non-haze image (d) Edges of haze image

Fig. 2. The edges of haze image and non-haze image.

To obtain the edge information of an image, it is necessary to choose a suitable method. There are many common methods for edge detection, such as Sobel operator, Kirsch operator, Laplacian operator, and Canny operator. Among them, the Canny operator is chosen. Canny edge detection algorithm is a multi-level edge detection algorithm developed by John F. Canny in 1986 [2]. This algorithm is considered by many to be the best edge detection algorithm. Compared with other edge detection algorithms, its accuracy in recognizing image edges is much higher and it has more accurate positioning of edge points. These advantages enable the algorithm to process blurry images, such as haze images. To use the Canny edge detection algorithm, the original image is first converted to a grayscale image. The algorithm consists of four steps: noise reduction, gradient calculation, non-maximum suppression, and double threshold edge tracking by hysteresis. After these steps, a binary edge image is obtained from the original image. Figure 2 shows the edges of a haze image and a non-haze image obtained by the Canny operator, clearly demonstrating that haze reduces image edges. Therefore, the edge feature of images can be used as another classification basis.

Dark Channel Feature. He *et al.* [8] proposed that in a non-haze image divided into multiple sub-blocks, at least one color channel of some pixels in each sub-block will have a very low value (nearly zero) in the non-sky region. This law is called the prior law of dark channel and the channel with the lowest value in the three color channels is called the dark channel. Conversely, in a haze area, the intensity of the dark channel is higher because of the influence of haze.

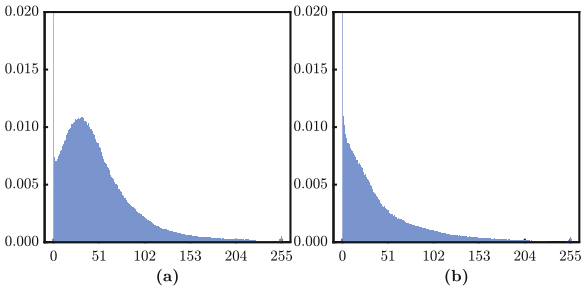

Fig. 3. Dark channel histograms of haze images and non-haze images. (a) Dark channel histogram of haze images and probability of 0 value is 0.2100 (b) Dark channel histogram of non-haze images and probability of 0 value is 0.5711

Therefore, this prior law can be used to distinguish whether the image contains haze or not. To obtain the dark channel of an image, perform according to the following formula:

$$J^{\text{dark}}(x) = \min_{y \in \Omega(x)} \left[\min_{c \in \{r,g,b\}} J^c(y) \right] \tag{3}$$

J^{dark} means dark channel value, $\Omega(x)$ means a local patch centered at x and J^c means value of each color channel. After conducting numerous experiments, a patch size of 15×15 is selected. Figure 3 displays the average histograms of the dark channel for 230 haze images and 270 non-haze images separately. There is a clear contrast between the dark channel histograms of haze and non-haze images, it can be seen that haze makes the distribution of the dark channel shift backward and reduces the proportion of pixels having zero dark channel value. Therefore, distinguishing between haze and non-haze images can be achieved by analyzing the dark channel histogram.

2.2 Classification Using SVM

SVM is a frequently used classifier in supervised learning. SVM developments started from Boser *et al.* [1] in 1992, this kind of SVM is known as the hard margin SVM. And in 1995, Cortes and Vapnik [6] improved SVM to the soft margin SVM in order to reduce the influence of noise and outliers by introducing slack variables. The soft margin SVM is the most popular and widely used SVM, which is also used in our classification task, given its strong performance with high dimensional data and small sample data. SVM algorithm aims to find the optimal hyperplane, which can not only separate two classes of samples correctly but also maximize the width of the gap between them. The widest gap is called optimal margin and the borderline instances are called Support Vectors [4]. For binary classification tasks, it is supposed that the training set comprises points of the form (x_i, y_i), $y_i \in \{-1, +1\}$, for $i = 1, 2, \ldots, m$, where $x_i \in \mathbb{R}^n$, n represents the number of features and m represents the number of points in the training

set. Then the hyperplane is set to be $\omega^T x + b = 0$. The hard margin SVM solves the following optimization problem to obtain the parameters ω, b:

$$\begin{aligned} &\min_{\omega,b} \tfrac{1}{2}\|\omega\|^2 \\ s.t. \quad &y_i\left(\omega^T x_i + b\right) \geq 1, i = 1, 2, \ldots, m \end{aligned} \tag{4}$$

Formula 4 represents the prime form of the hard margin SVM which can be solved using Lagrangian Multipliers. The dual form is as follows, where α is vector of dual variables α_i:

$$\begin{aligned} &\max_{\alpha} -\tfrac{1}{2}\sum_{i=1}^{m}\sum_{j=1}^{m}\alpha_i\alpha_j y_i y_j x_i^T x_j + \sum_{i=1}^{m}\alpha_i \\ s.t. \quad &\sum_{i=1}^{m}\alpha_i y_i = 0, \alpha_i \geq 0, i = 1, 2, \ldots, m \end{aligned} \tag{5}$$

As for the soft margin SVM, to reduce the impact of noise and outliers, slack variables are introduced as $\xi_i = \max[0, 1 - y_i(\omega^T x_i + b)]$. This modification changes the prime form to:

$$\begin{aligned} &\min_{\omega,b} \tfrac{1}{2}\|\omega\|^2 + C\sum_{i=1}^{m}\xi_i \\ s.t. \quad &y_i\left(\omega^T x_i + b\right) \geq 1 - \xi_i, i = 1, 2, \ldots, m \end{aligned} \tag{6}$$

C is the penalty parameter to control the punishment of outliers, and it is a hyper-parameter that needs to be set in advance and adjusted during application. Additionally, the dual form of the problem is obtained:

$$\begin{aligned} &\max_{\alpha} -\tfrac{1}{2}\sum_{i=1}^{m}\sum_{j=1}^{m}\alpha_i\alpha_j y_i y_j x_i^T x_j + \sum_{i=1}^{m}\alpha_i \\ s.t. \quad &\sum_{i=1}^{m}\alpha_i y_i = 0, 0 \leq \alpha_i \leq C, i = 1, 2, \ldots, m \end{aligned} \tag{7}$$

For non-linear separable data, the soft margin SVM may not perform well, so kernel functions are utilized. Kernel functions can transform the low-dimensional space to high-dimensional space where the feature is linearly separable. SVM with kernel function doesn't need to calculate the mapping of feature to high dimensional space; instead, it only needs to calculate the inner product of the mapping. Therefore, the cost of using SVM with kernel functions is lower than that of other non-linear classifiers.

To mitigate the impact of noise and outliers, the soft margin SVM is chosen to be used. Given the small scale of our training set, reducing the dimension of the feature vector is crucial for improving classification results. Thus, for the color feature and the dark channel feature, 256-dimensional histograms are simplified to 16-dimensional histograms. Additionally, since the edge feature histogram reflects a binary image with only two values, the 0 value of the histogram is obtained. After that, these features are integrated together as a 65-dimention final feature which is utilized in SVM.

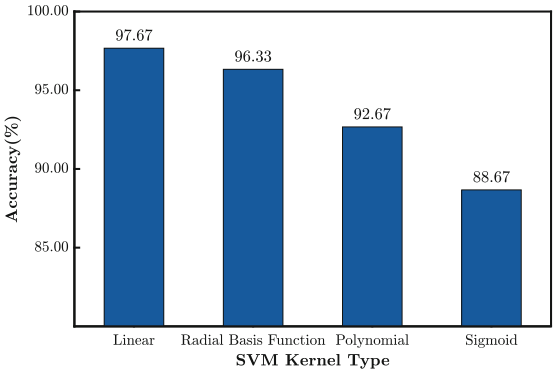

Fig. 4. Performance of SVM using different kernel.

3 Experiments

3.1 Dataset and Experimental Settings

The training set comprises 500 endoscopic images, including 230 haze images and 270 non-haze images, which is obtained from an endoscopic surgery video. Additionally, a test set of 300 images including 150 haze images and 150 non-haze images is obtained from another video. The SVM model used is C-SVM in LIBSVM [3], and the SVM classifier is trained using the feature set and labels obtained from the training set. The parameters are chosen through 10-fold cross-validation. Subsequently, the accuracy rate is assessed by inputting the feature set of the test set into the SVM model and comparing the classification results with the labels. All experiments are conducted on a PC with a CPU (Intel i7 12700H, 2.30 GHz). The input endoscopic images, which are manually labeled, have a resolution of 1920×1080.

3.2 Classification Results with Different Kernel and Dimension

The classification effect of different kernel functions, including linear function, polynomial function, radial basis function, and sigmoid function is compared to select the appropriate kernel function for SVM. The selected kernel function is the linear function, as it achieves the highest classification accuracy, as shown in Fig. 4. Next, various dimensions of histograms are contrasted. Figure 5 shows how changes in histogram dimensions from 8 to 256 affect classification performance. Dimensions of 8, 16, 32, 64, 128, and 256 are chosen to ensure that all the modified columns consist of an integral number of columns. The results indicate that the dimension of the histogram have little impact on classification accuracy after each histogram's dimensions are set to 16. Consequently, to achieve higher accuracy and lower dimension, 16 dimensions is selected for each histogram.

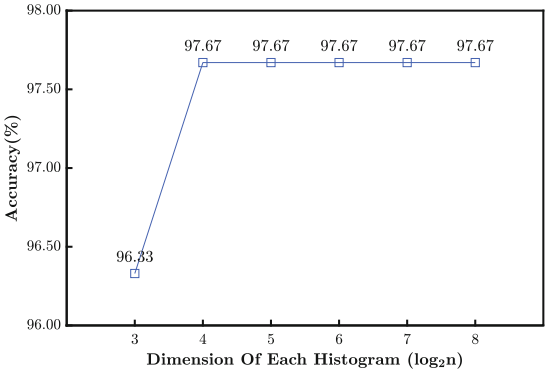

Fig. 5. Performance of features with different dimensions.

Table 1. Result with Different Fusions of Features

Features			Accuracy (%)
Color	Edge	Dark Channel	
✓			92.33
	✓		73.67
		✓	96.33
✓	✓		93.33
✓		✓	95.33
	✓	✓	97.00
✓	✓	✓	97.67

3.3 Classification Results with Different Weights of Features

Since the final feature is fused with three kinds of features, the importance of each kind of feature is verified. In Table 1, the classification accuracy with fusion of different features is given. The results indicate that fusing all three features result in better performance than using a single or two features. The weight of each feature is also varied to search for the optimal fusion strategy, and classification results are compared as shown in Table 2, with the sum of weights set to 1 and the weights of the three kinds of features changed separately. It is found when the weights of the color, edge and dark channel features are assigned to 1/6, 1/2 and 1/3, the highest accuracy 98.67% is achieved on the test set.

4 Discussion

The main challenge of classifying endoscopic haze images is selecting features that can best distinguish between haze and non-haze images. Therefore, three

Table 2. Results with Different Weights of Features

Weights of Features			Accuracy (%)
Color	Edge	Dark Channel	
1/3	1/3	1/3	97.67
1/4	1/4	1/2	98.33
1/4	1/2	1/4	97.67
1/2	1/4	1/4	96.67
1/3	1/6	1/2	98.00
1/3	1/2	1/6	97.67
1/2	1/6	1/3	97.00
1/2	1/3	1/6	96.33
1/6	1/3	1/2	98.33
1/6	1/2	1/3	98.67

types of image features are chosen based on the characteristics of endoscopic haze images. First, the physical knowledge that haze can reduce the saturation of images and increase the brightness of the images is considered. Hence, the HSI color model which can represent the saturation and brightness of the image is chosen as the first kind of feature. The second kind of feature is the edge information of images, as haze tends to blur edges. Finally, the dark channel feature is chosen as the third kind of feature, which is commonly used in dehazing tasks and can tell the difference between haze and non-haze images well. Experiments are conducted to verify the effectiveness of these features.

Figure 6 and Fig. 7 show the confusion matrices for different weights. Figure 6 indicates that using a single edge feature results in the worst classification effect, while a single dark channel feature leads to the best classification effect. Fusing all three features achieves a better result than using one or two features alone, demonstrating the importance of all three features. From Fig. 7, it can be inferred that assigning high weights to the dark channel and edge features and low weights to the color feature improves the classification effect. This may be owing to the low dimensionality of the edge feature, necessitating higher weights to avoid ignoring it. Conversely, the color feature has a high dimensionality, requiring lower weights. Additionally, because of the good performance of the dark channel feature in classification, its weight should be high.

To prove feasibility and effectiveness, our method is compared with other methods. Both traditional ML-based methods and CNN-based methods are employed for the classification task. In CNN based methods, ResNet50 [9] and VGG16 [14] are chosen. Owing to the small scale of our training set, the ResNet50 model which is pre-trained on the ImageNet dataset is fine-tuned by changing the fully connected layer's parameters. The same was done for VGG16. The results, shown in Table 3, indicate an accuracy of 97.00% with ResNet50 and 93.67%

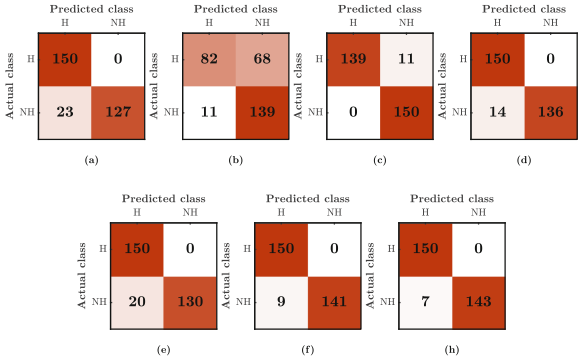

Fig. 6. Confusion matrices of fusions with different features. (a) color feature (b) edge feature (c) dark channel feature (d) color feature and dark channel feature (e) color feature and edge feature (f) edge feature and dark channel feature (g) color feature, edge feature, and dark channel feature

Table 3. Results with different methods

Methods	Accuracy (%)	Precision (%)	Recall (%)
KNN	94.67	90.36	100.0
RF	92.67	87.21	100.0
VGG16	94.67	92.45	98.00
ResNet50	97.00	94.90	99.33
Ours	98.67	98.03	99.33

with VGG16 on the test set, both lower than our SVM method. In addition, our method outperforms them in precision and recall values. This may be because our training set is small and the feature extracted is approximately linearly separable. Other traditional ML-based methods like KNN and Random Forest (RF) are also used, using the same features as SVM. The results, presented in Table 3, show that KNN achieves an accuracy of 94.67% and RF achieves an accuracy of 92.67%, both lower than our SVM method. However, these two methods have higher recall values than SVM. That may be because these two methods pay more attention to outliers and noise, which result in higher recall and lower precision. In summary, our SVM method is proved to be effective and feasible.

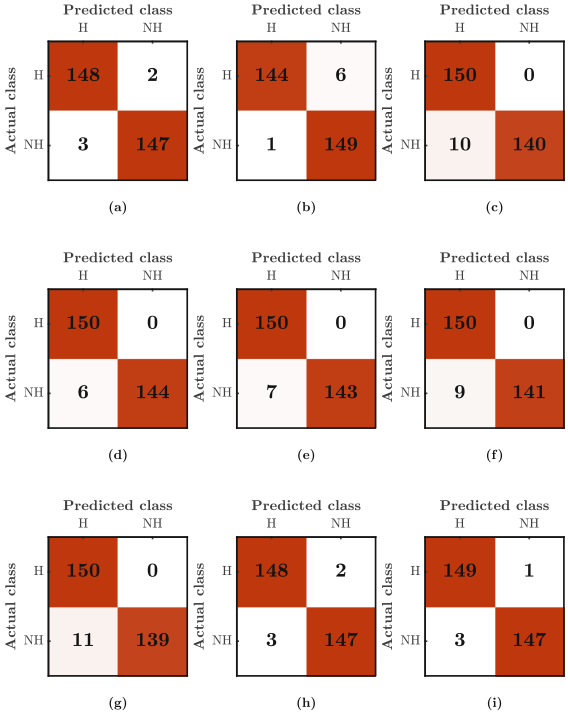

Fig. 7. Confusion matrices of features with different weights. The proportion of weights of color feature, edge feature, and dark channel feature (w_c: color feature, w_e: edge feature, w_d: dark channel feature): (a) w_c: w_e: $w_d = 1 : 1 : 2$ (b) w_c: w_e: $w_d = 1 : 2 : 1$ (c) w_c: w_e: $w_d = 2 : 1 : 1$ (d) w_c: w_e: $w_d = 2 : 1 : 3$ (e) w_c: w_e: $w_d = 2 : 3 : 1$ (f) w_c: w_e: $w_d = 3 : 1 : 2$ (g) w_c: w_e: $w_d = 3 : 2 : 1$ (h) w_c: w_e: $w_d = 1 : 2 : 3$ (i) w_c: w_e: $w_d = 1 : 3 : 2$

5 Conclusion

This paper proposes a novel SVM-based approach for effectively distinguishing between haze and non-haze endoscopic images. Our method selects three kinds of features (i.e., color, edge, and dark channel) based on the unique characteristics of endoscopic haze images. These features can be fused with a suitable strategy to recognize the haze in endoscopic images effectively, achieving superior performance than existing methods. This method can be applied before dehazing algorithms to improve their efficacy on endoscopic images, potentially improving surgical accuracy and reducing surgical risks.

Acknowledgements. This work was supported in part by the National Natural Science Foundation of China under Grant 62003343, Grant 62222316, Grant U1913601, Grant 62073325, Grant U20A20224, and Grant U1913210; in part by the Beijing Natural Science Foundation under Grant M22008; in part by the Youth Innovation Promotion Association of Chinese Academy of Sciences (CAS) under Grant 2020140; in part by the CIE-Tencent Robotics X Rhino-Bird Focused Research Program.

References

1. Boser, B.E., Guyon, I.M., Vapnik, V.N.: A training algorithm for optimal margin classifiers. In: Proceedings of the Fifth Annual Workshop on Computational Learning Theory, pp. 144–152 (1992)
2. Canny, J.: A computational approach to edge detection. IEEE Trans. Pattern Anal. Mach. Intell. **6**, 679–698 (1986)
3. Chang, C.C., Lin, C.J.: LIBSVM: a library for support vector machines. ACM Trans. Intell. Syst. Technol. (TIST) **2**(3), 1–27 (2011)
4. Chauhan, V.K., Dahiya, K., Sharma, A.: Problem formulations and solvers in linear SVM: a review. Artif. Intell. Rev. **52**(2), 803–855 (2019)
5. Chincholkar, S., Rajapandy, M.: Fog image classification and visibility detection using CNN. In: Pandian, A.P., Ntalianis, K., Palanisamy, R. (eds.) ICICCS 2019. AISC, vol. 1039, pp. 249–257. Springer, Cham (2020). https://doi.org/10.1007/978-3-030-30465-2_28
6. Cortes, C., Vapnik, V.: Support-vector networks. Mach. Learn. **20**, 273–297 (1995)
7. Guo, L., et al.: Haze image classification method based on AlexNet network transfer model. J. Phys.: Conf. Ser. **1176**, 032011 (2019)
8. He, K., Sun, J., Tang, X.: Single image haze removal using dark channel prior. IEEE Trans. Pattern Anal. Mach. Intell. **33**(12), 2341–2353 (2010)
9. He, K., Zhang, X., Ren, S., Sun, J.: Deep residual learning for image recognition. In: Proceedings of the IEEE Conference on Computer Vision and Pattern Recognition, pp. 770–778 (2016)
10. Pal, T., Halder, M., Barua, S.: Multi-feature based hazy image classification for vision enhancement. Procedia Comput. Sci. **218**, 2653–2665 (2023)
11. Pei, Y., Huang, Y., Zhang, X.: Consistency guided network for degraded image classification. IEEE Trans. Circuits Syst. Video Technol. **31**(6), 2231–2246 (2020)
12. Satrasupalli, S., Daniel, E., Guntur, S.R., Shehanaz, S.: End to end system for hazy image classification and reconstruction based on mean channel prior using deep learning network. IET Image Process. **14**(17), 4736–4743 (2020)
13. Shrivastava, S., Thakur, R.K., Tokas, P.: Classification of hazy and non-hazy images. In: Proceeding of 2017 International Conference on Recent Innovations in Signal processing and Embedded Systems (RISE), pp. 148–152 (2017)
14. Simonyan, K., Zisserman, A.: Very deep convolutional networks for large-scale image recognition. arXiv preprint arXiv:1409.1556 (2014)
15. Wan, J., Qiu, Z., Gao, H., Jie, F., Peng, Q.: Classification of fog situations based on gaussian mixture model. In: Proceeding of 2017 36th Chinese Control Conference (CCC), pp. 10902–10906 (2017)
16. Yu, X., Xiao, C., Deng, M., Peng, L.: A classification algorithm to distinguish image as haze or non-haze. In: Proceeding of 2011 Sixth International Conference on Image and Graphics, pp. 286–289 (2011)
17. Zhang, Y., Sun, G., Ren, Q., Zhao, D.: Foggy images classification based on features extraction and SVM. In: Proceeding of 2013 International Conference on Software Engineering and Computer Science, pp. 142–145 (2013)